LDL and HDL transfer rates across peripheral microvascular endothelium agree with those predicted for passive ultrafiltration in humans

C. Charles Michel,* M. Nazeem Nanjee,† Waldemar L. Olszewski,§ and Norman E. Miller[1],**

Department of Bioengineering,* Imperial College, London, UK; Cardiovascular Genetics Unit,† University of Utah School of Medicine, Salt Lake City, UT; Department of Surgical Research and Transplantology,§ Medical Research Centre, Polish Academy of Sciences, Warsaw, Poland; and Magdalen College,** University of Oxford, Oxford, UK

Abstract The mechanisms by which LDLs and HDLs cross the vascular endothelium from plasma into interstitial fluid are not understood, and have never been studied in humans in vivo. We determined whether the plasma-to-lymph clearance rates of LDL and HDL conform with those predicted by passive ultrafiltration through intercellular pores, or if it is necessary to invoke an active process such as receptor-mediated transcytosis. Plasma and afferent peripheral lymph were collected under steady-state conditions from 30 healthy men, and assayed for seven globular proteins of molecular radii 2.89–8.95 nm, complement C3, and apo AI, apo AII, and apo B. Plasma-to-lymph clearance rates of the seven proteins fitted the relation expected for molecules of their size when transported through two populations of pores of radius 4.95 and 20.1 nm. The same model parameters were then found to accurately predict the clearance rates of both HDL and LDL. The apparent clearance of complement C3, previously shown to be secreted by cultured endothelium, exceeded that predicted by the model. We conclude that the transport of HDL and LDL from plasma into interstitial fluid across the peripheral vascular endothelium in healthy humans can be explained by ultrafiltration without invoking an additional active process such as transcytosis.—Michel, C. C., M. N. Nanjee, W. L. Olszewski, and N. E. Miller. **LDL and HDL transfer rates across peripheral microvascular endothelium agree with those predicted for passive ultrafiltration in humans. *J. Lipid Res.* 2015.** 56: **122–128.**

Supplementary key words low density lipoprotein • high density lipoprotein • transcytosis

Plasma lipoproteins transport lipids between different tissues of the body. Mature particles have a central core of neutral lipids enclosed within a bilayer of phospholipids in association with cholesterol and apos. The largest particles, chylomicrons and VLDLs, are limited in distribution to blood and metabolized at the luminal surface of vascular endothelium by lipoprotein lipase. By contrast, the LDLs and HDLs move between plasma and interstitial fluid as they transport lipids to and from different cell types. Each LDL particle contains a single molecule of apoB100 (apo B) (1, 2). The principal protein component of all HDL particles is apo AI, which usually accounts for about 70% of total HDL protein mass. Some HDLs also contain apo AII as the second most abundant protein (3). Studies of human afferent peripheral lymph have shown that the concentrations of apo AI and apo AII in normal human interstitial fluid average about one-fifth of those in plasma (4–6), while lymph apo B concentration averages only one-tenth (4, 7). The ratio of HDL to LDL particles in interstitial fluid has been estimated to average about 50:1 in healthy humans (4, 8).

The striking differences in lipoprotein concentrations between plasma and interstitial fluid, combined with their roles in atherosclerosis, highlight the importance of understanding the mechanisms by which they move into and out of the extravascular compartment. By analyzing data on adipokines of different molecular size, Miller et al. (9) showed that the principal pathway by which a macromolecule leaves the interstitium of peripheral tissues in humans is determined by its size, the proportion leaving via capillaries decreasing and that via the lymphatic system increasing, as molecular radius rises. As proteins of radius $\geqslant$3.2 nm were found to leave entirely in lymph, it is reasonable to assume that this applies also to LDL and HDL, given that their radii greatly exceed this figure (10, 11). This interpretation agrees with recent studies of HDL transport via the lymphatic system in mice (12).

The mechanisms by which HDL and LDL are transported from plasma into interstitial fluid are not understood. Two

This study was supported by the British Heart Foundation. The authors declare no financial conflicts of interest.

Manuscript received 24 September 2014 and in revised form 10 November 2014.

Published, JLR Papers in Press, November 14, 2014
DOI 10.1194/jlr.M055053

[1]To whom correspondence should be addressed.
e-mail: n.e.miller@btinternet.com

processes are possible: an active transport mechanism such as receptor-mediated transcytosis (13) or ultrafiltration through intercellular pores in the endothelium, a pathway that is thought to be available to all macromolecules below a critical size (14). Evidence for receptor-mediated LDL transport across the endothelium of the blood-brain barrier has been obtained in vitro (15). However, there is no published evidence for a similar process in other vessels. Vlodavsky et al. (16) reported that cultured bovine endothelial cells bound, internalized, and degraded LDL during logarithmic growth, while confluent cells bound but did not internalize the particles. Measurements of LDL transport across microvascular endothelia in the peripheral circulation of animals in vivo have yielded results consistent with ultrafiltration (17–19), but there have been no similar studies in humans. Transcytosis of HDL through endothelial cells has been described in tissue culture, apparently by mechanisms involving the same ABCG1 and SR-B1 receptors implicated in the movement of cholesterol into and out of other cell types (20–22).

To study the mechanisms of trans-endothelial transport of LDL and HDL in humans in vivo, we collected afferent peripheral lymph from healthy subjects, and compared the concentrations of apo B, apo AI, apo AII, and seven globular proteins of differing sizes with those in plasma. The plasma-to-lymph clearances of the seven proteins conformed to those predicted by the theory (23, 24) of ultrafiltration and diffusion through two populations of pores. The same model parameters were then found to accurately predict the observed clearance rates of both LDL and HDL, supporting the hypothesis that their transport is also limited to passive ultrafiltration.

METHODS

Subjects

Studies were carried out in 30 healthy males not taking medication or alcohol (**Table 1**). A medical history was taken from all subjects, and each was given a clinical examination. Blood samples were examined by routine clinical chemistry for renal, hepatic, and endocrine dysfunction, and for recreational drugs. The study conformed to the principles of the Declaration of Helsinki, and was approved by the ethics committees of St. Bartholomew's Hospital and London Bridge Hospital, London, UK. All subjects gave informed consent.

Clinical procedures

Subjects were admitted to a metabolic ward in London Bridge Hospital, London, UK and placed on a normal solid diet designed to maintain constant body weight. Twenty-four or 48 h later, a prenodal (afferent) lymph vessel in the lower leg was cannulated in a surgical theater under local anesthesia and sterile conditions, as described elsewhere (4). A sterile siliconized polyethylene cannula was left in place, draining into a 2 ml polypropylene vial strapped to the leg, and the volunteer returned to the ward. The samples for study were collected during 2–4 h between 6:00 and 10:00 AM before breakfast, after the subjects had been supine and fasting since 10:00 PM or earlier the previous night. The volume of lymph was measured, the sample was centrifuged (30 min, 1,500 *g*, 4°C), and aliquots were dispensed into cryovials for storage at −80°C. Antecubital venous blood was drawn at the midpoint of the lymph collection. Ambient air temperature was controlled by air conditioning. No cannula became blocked, and no local wound infection occurred. When the collection was complete, the cannula was withdrawn and a dressing applied.

Analytical methods

Plasma cholesterol and triglycerides were assayed enzymatically (25). Pairs of plasma and lymph samples from each subject were analyzed together for apo AI, apo AII, and apo B, complement C3, and seven proteins covering a wide range of molecular radii (albumin, α1-acid glycoprotein, α1-antitrypsin, transferrin, immunoglobulin G, antithrombin III, and α2-macroglobulin). None of the globular proteins are known to be secreted by the endothelia of adipose tissue, skin, or connective tissue, and all are thought to be transported from plasma to interstitial fluid by passive ultrafiltration (23, 24). Plasma proteins were quantified by rocket immunoelectrophoresis using polyclonal antisera (International Immunology Corp., Murrieta, CA), and apos by liquid phase double antibody radio-immunoassays (4). Samples and standards were assayed in duplicate with intra-assay coefficients of variation of <6.0% for proteins and <2.5% for apos.

Calculations

We first tested the hypothesis that the plasma-to-lymph clearances of the seven globular proteins fitted the two-pore model of trans-endothelial transport described by others (14, 23), in which most fluid is filtered through a large number small channels and a small fraction through a smaller number of large channels, and estimated the model parameters. We then examined the accuracy with which the same model predicted the observed clearances of LDL and HDL, using the apo concentrations as markers of particle number and published data on mean particle radii. Finally, as a positive control, we tested the hypothesis that the apparent clearance rate of complement C3 exceeds that predicted by the model, given that it is known to be secreted by cultured endothelium (26). The molecular masses and molecular (Stokes-Einstein) radii of the proteins and the mean particle radii of HDL and LDL are given in **Table 2**. The molecular radii of the proteins were calculated from their molecular masses using the expression of Rippe and Stelin (27). The mean radii of the lipoproteins were those obtained by other investigators by NMR in very large samples of healthy subjects (10, 11).

TABLE 1. Clinical characteristics of the subjects and lymph flow rates

	Age (years)	Weight (kg)	BMI (kg/m^2)	Cholesterol (mmol/l)	Triglycerides (mmol/l)	HDL Cholesterol (mmol/l)	Lymph Flow (ml/h)
Mean ± SD	31.3 ± 11.5	77.3 ± 12.5	23.5 ± 3.1	4.8 ± 0.9	1.10 ± 0.32	1.08 ± 0.27	0.82 ± 0.87[a]
Range	21–69	50–105	18.5–31.0	3.3–7.1	0.40–1.75	0.71–1.61	0.05–4.10

Data are from 30 healthy men. In all subjects fasting blood glucose was within the reference range, 4–8 mmol/l.
[a]Median, 0.60 ml/h.

TABLE 2. Molecular masses, molecular radii, and concentrations of the seven globular plasma proteins, LDL, HDL, and complement C3 in thirty healthy men

	Molecular Mass (kDa)	Molecular Radius[a] (nm)	Concentration (mg/dl) (mean ± SEM)	
			Plasma	Lymph
α1-Acid glycoprotein	40	2.89	94.6 ± 3.0	38.7 ± 1.9
α1-Antitrypsin	55	3.26	131.0 ± 3.9	49.5 ± 2.7
Antithrombin III	58	3.33	5.7 ± 0.1	2.0 ± 0.1
Albumin	66	3.50	4722 ± 64	1665 ± 83
Transferrin	77	3.72	216.3 ± 8.4	75.4 ± 4.8
Immunoglobulin G	150	4.81	1158 ± 40	215 ± 24
α2-Macroglobulin	750	8.95	304 ± 35	34.7 ± 3.5
LDL	—	10.7	—	—
Apo B	—	—	82.4 ± 4.1	7.7 ± 0.47
HDL	—	4.5	—	—
Apo AI	—	—	130 ± 6.1	26.7 ± 1.5
Apo AII	—	—	33.1 ± 1.2	6.8 ± 0.43
Complement C3	180	5.16	34.8 ± 1.4	8.3 ± 0.7

[a]Molecular radii of the plasma proteins were calculated using the Stokes-Einstein equation. Lipoprotein particle radii are those obtained by NMR, and were taken from the literature, as described under Methods.

The plasma-to-lymph clearances of the molecules were estimated from lymph flow, J_L, and their concentrations in lymph and plasma (C_L and C_P):

$$\text{Clearance} = J_L \cdot \frac{C_L}{C_P} \qquad \textit{(Eq. 1)}$$

The ratio of the concentration of a spherical molecule or particle in plasma to that in interstitial fluid was calculated on the assumption that it passes by ultrafiltration and diffusion through two populations of water-filled channels in the endothelium, modeled as cylindrical pores with radii of molecular dimensions, one consisting of numerous channels with radii in the range 4.0–5.5 nm (small pores), and the second consisting of relatively few channels with radii in the range 18–40 nm (large pores). Knowing the radii of the molecules or particles, the radii of the pores, and the rate of fluid filtration through them, the ratio C_L/C_P in equation 1 can be replaced by a ratio of membrane coefficients. Thus, the overall clearance of a molecule of radius a is given by:

$$\text{Clearance through large pores plus clearance through small pores} = J_L \frac{C_L}{C_P} = \alpha_L J_L \frac{(1-\sigma_L)}{\left(1-\sigma_L e^{-Pe(L)}\right)} + (1-\alpha_L) J_L \frac{(1-\sigma_S)}{\left(1-\sigma_S e^{-Pe(S)}\right)} \qquad \textit{(Eq. 2)}$$

where α_L is the fraction of lymph formed by ultrafiltration through large pores; σ_L and σ_S are the reflection coefficients of the molecule at the large and small pores respectively; and $Pe(L)$ and $Pe(S)$ are the Peclét numbers of transport for the molecule in the large and small pores, respectively.

The reflection coefficients are determined by the radii of the molecules and the radii of the large pores (R_L) and small pores (R_S):

$$\sigma_{L(S)} = \left[1 - \left(1 - \frac{a}{R_{L(S)}}\right)^2\right]^2 \qquad \textit{(Eq. 3)}$$

where $\sigma_{L(S)}$ is either σ_L or σ_S, and $R_{L(S)}$ is either R_L or R_S (28).

The Peclét numbers can be thought of as the ratio of the convective velocity of the molecule within a pore to its diffusive velocity. Thus, they are determined not only by a function of a/R, but also by the flow through the pore. The latter can be calculated from the pore radius, the solvent viscosity (η) and the net hydraulic pressure difference (ΔP) driving fluid through the pore:

$$Pe_{L(S)} = \frac{R_L^2 \Delta P\left(1-\sigma_{L(S)}\right)}{8\eta D \cdot f\left(a/R_{L(S)}\right)} \qquad \textit{(Eq. 4)}$$

D is the free diffusion coefficient of the molecule, and can be calculated from the Stokes-Einstein relation and a. The function $f(a/R_{L(S)})$ is given by:

$$f\left(a/R_{L(S)}\right) = \left(1 - a/R_{L(S)}\right)^2 \cdot \left\{1 - 2.10\left(a/R_{L(S)}\right) + 2.09\left(a/R_{L(S)}\right)^3 - 0.95\left(a/R_{L(S)}\right)^5\right\} \qquad \textit{(Eq. 5)}$$

The evaluation of the parameters of the curve relating plasma-to-lymph clearance to molecular radius started with the assumption that the largest particles can pass through the large pores only. Thus, their clearance indicates the fraction of the lymph flow that derives from passage through the large pores (α_L). Furthermore, as large molecules in large pores (radii, 18–40 nm) are transported almost entirely by convection, Pe is considerably greater than one, so that e^{-Pe} approaches zero (second term on the right hand side of equation 2). The clearance of these large particles then simplifies to:

$$\text{Total clearance} = \text{large pore clearance} = \alpha_L J_L (1-\sigma_L) \qquad \textit{(Eq. 6)}$$

Assuming R_L lies between 18 and 40 nm, the decline of the clearances of the two largest particles (α_2-macroglobulin and LDL) with increasing radius and the initial estimate of α_L can be iterated to obtain better estimates of α_L, σ_L, and R_L using equations 3 and 6. With values for these parameters, the relation between clearance of all molecules and particles through the large pores can be calculated. This is the first term on the right hand side of equation 2. Clearance through the small pores (second term on the right hand side of equation 2) can now be estimated by subtracting the large pore clearance from the total clearance of the smaller plasma proteins to obtain the fraction of the clearance of these molecules that is through the small pores. Equations 3–5 are then used to find the value of R_S that offers the best fit to these values of small pore clearance.

In estimating the Peclét number through the large pores, ΔP was assumed to equal the mean microvascular pressure, which has been measured in the feet of supine humans (~30–40

cmH_2O) (29, 30), on the grounds that the effective osmotic pressure exerted by plasma macromolecules across the large pores would be negligible, because the reflection coefficients of proteins contributing most to this would be very low. This assumption cannot be made for the osmotic pressures exerted across the small pores. Here, the effective colloidal osmotic pressure difference opposing filtration is comparable with the mean hydrostatic pressure difference that drives it. For an initial estimate of the colloid osmotic pressure difference across the small pores, the plasma colloid osmotic pressure was calculated from the total protein concentration using the expression of Landis and Pappenheimer (31) and multiplied by 0.75, which was taken as an estimate of the square of the mean reflection coefficient of the plasma proteins (32). Once a rough estimate of R_S had been made, the values of σ_S of the plasma proteins could be calculated for the proteins of different molecular radii (equation 3), and these used to estimate the steady state osmotic pressure differences across the small pores for each molecule. With Π_P indicating the plasma colloid osmotic pressure of the major plasma proteins, the effective colloid osmotic pressure difference exerted by all plasma proteins across the small pores under steady-state conditions ($\sigma_S\Delta\Pi_S$) was calculated from the expression (33, 34):

$$\sigma_S\Delta\Pi_S = \sum \sigma_S^2\Pi_P \frac{\left(1-e^{-Pe(s)}\right)}{\left(1-\sigma_s e^{-Pe(S)}\right)} \qquad \textit{(Eq. 7)}$$

This value of $\sigma_S\Delta\Pi_S$ was subtracted from the initial estimate of the mean hydrostatic pressure difference, and the calculation of $Pe(S)$ repeated. Only a couple of iterations were needed for a constant value of R_S to be reached. A similar iterative procedure was initially used to assess the influence of the estimated value of ΔP across the large pores upon the final estimate of R_L, but found to be unnecessary.

Statistical analysis

The best nonlinear curve relating clearance to molecular radius (equation 2) was obtained by adjusting the values of α_L, R_L, and R_S to minimize the sum of the squares of the differences between measured and predicted values of clearance. First, values of α_L and R_L were adjusted to fit the curve to proteins with the largest molecular radii. Subsequently, values of R_S were adjusted to obtain the best fit for the entire curve. Changes in R_L and R_S were made in successive 2, 1, and 0.5 nm steps to establish the minimum. Changes in α_L were made in steps of 0.02 and 0.01.

RESULTS

The concentrations in plasma and lymph of the seven globular proteins, three apos and complement C3 are given in Table 2. **Figure 1** shows the curvilinear relation between clearance and molecular radius predicted by the two-pore theory of microvascular permeability when $\alpha_L = 0.20$, $R_L = 20.1$ nm, and $R_S = 4.95$ nm, the parameters that gave the best fit for the seven globular proteins. The mean observed clearance rates of the proteins are represented by the symbols, and the means and SEMs are provided in the legend. **Figure 2** shows the same curve, on which are now superimposed the mean observed clearance rates of LDL (apo B) and HDL (two values, based on the apo AI or apo AII data). The means and SEMs are again provided in the legend. It is evident that the clearances of both LDL and HDL were accurately predicted by the same two-pore model that gave the best fit for the seven proteins. It is also seen that the mean clearance of HDL obtained using apo AII was essentially identical to that obtained using apo AI. Figure 2 additionally shows that the clearance rate of complement C3, known to be secreted by cultured endothelium (26), was much greater than that predicted by the curve for a molecule of its size.

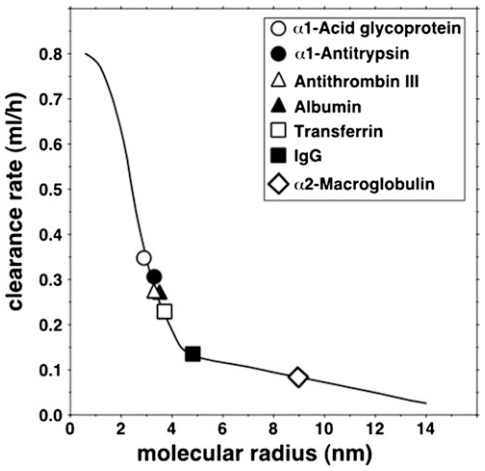

Fig. 1. Relation of plasma-to-lymph clearance rates of seven globular plasma proteins to their molecular radii. The continuous line is the curve predicted by the two-pore model of ultrafiltration with the following parameters: small pore radius, 4.95 nm; large pore radius, 20.1 nm; numerical ratio of small to large pores, 7,700 to one. The symbols represent the mean measured clearances of the proteins. Mean clearances and SEMs (ml/h) were as follows: α1-glycoprotein, 0.345 ± 0.060; α1-antitrypsin, 0.306 ± 0.060; antithrombin III, 0.270 ± 0.058; albumin, 0.271 ± 0.055; transferrin, 0.228 ± 0.055; immunoglobulin G, 0.135 ± 0.020; α2-macroglobulin, 0.086 ± 0.013.

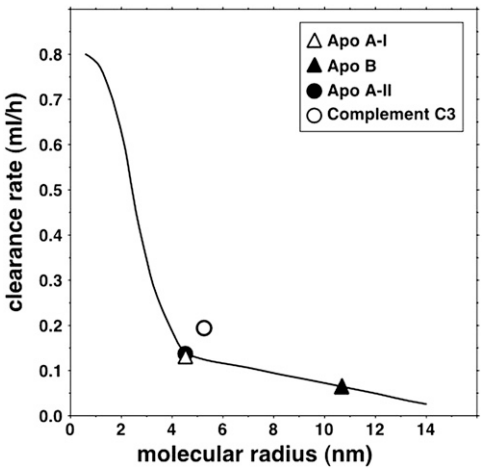

Fig. 2. Plasma-to-lymph clearance rates of LDL, HDL, and complement C3 shown relative to the curve of clearance versus molecular radius previously obtained using the data on globular plasma proteins. Mean clearances and SEMs (ml/h) were as follows: LDL as apo B, 0.056 ± 0.009; HDL as apo AI, 0.116 ± 0.016; HDL as apo AII, 0.119 ± 0.018; complement C3, 0.190 ± 0.044.

When the clearance data from the subjects were analyzed individually, they conformed to the same pattern with some variation between subjects in the values of the parameters.

DISCUSSION

This is the first study of the trans-endothelial transport of either LDL or HDL in humans. It was carried out in two stages. In the first stage, we examined the clearance rates from plasma to interstitial fluid of seven plasma proteins that are considered (31) to cross the endothelium in peripheral tissues exclusively by passive ultrafiltration through intercellular pores. We found that the relation of clearance to molecular size, measured as Stokes-Einstein radius, was consistent with a two-pore model of ultrafiltration similar to that described by others (14, 23, 24), in which water and water-soluble molecules are carried through the endothelium by ultrafiltration and diffusion through a large number of small pores in parallel with a much smaller number of larger pores. Our analysis indicated that in the human leg, the small pores have a mean radius of 4.95 nm, and the large pores one of 20.1 nm. With 20% of lymph being derived by passage of water through the larger pores, these figures suggest that, on average, there are 7,700 small pores for each large pore in this site. In the second stage, we studied the precision with which the same model parameters predicted the clearance rates of HDL and LDL in the same subjects. We found that the observed clearance rates of both lipoproteins agreed well with those predicted by the model. By contrast, the clearance of complement C3 exceeded that predicted by the model, consistent with the observation that this protein is actively secreted by cultured endothelial cells (26).

Our findings indicate that the plasma-to-lymph transport of both LDL and HDL is limited to the same process of passive ultrafiltration that mediates the transport of the seven globular proteins, as any additional contributions from active processes would have raised the observed clearance rates to values exceeding those predicted by the model. Our conclusion with respect to LDL is in agreement with those of animal experiments in vivo (17–19). There have been no similar studies of trans-endothelial HDL transport in animals. In cell culture, HDL has been reported to be transported through endothelial cells by transcytosis after binding to one or another of several types of cell surface receptor (20–22). Our findings do not exclude this possibility, but suggest that if transcytosis occurs at all in healthy humans in vivo, it is not quantitatively significant. Our results are also consistent with the extremely low concentrations in human peripheral lymph of VLDLs (4), whose average radius is more than twice that of LDLs (11).

Renkin (35) has pointed out that if fluid within a caveola at the luminal surface of the endothelium were to equilibrate with plasma before budding off to form a vesicle, the concentrations of macromolecules in the vesicular fluid would be lower than in plasma. This is a consequence of the macromolecules being excluded from the region of fluid close to the internal surface of the vesicle. As larger molecules would have a greater volume of exclusion than smaller ones, the effect would convey a degree of size selectivity to any transcytosis resulting from nonspecific pinocytosis. However, this consideration does not apply to receptor-mediated transcytosis.

Our calculations assumed that no synthesis or catabolism of LDL or HDL occurs while the lipoproteins are in the extracellular matrix of the tissues drained by the lymph vessel (adipose tissue, connective tissue, and skin). This is in line with current knowledge of their metabolism. In humans, all three measured apos are exclusively splanchnic in origin (1, 36), while studies using LDL and HDL tagged with nondegradable markers in animals have shown there is little endocytosis of either lipoprotein in peripheral tissues (37–39). A second assumption was that any binding of lipoproteins to the extracellular matrix is in equilibrium with the corresponding lipoproteins in interstitial fluid.

For the calculation of LDL clearance, we used apo B concentration as a marker of LDL particle number in the knowledge that each particle contains a single molecule of apo B (1). Although VLDL particles also contain one apo B molecule, they are present only in extremely low concentration in normal human lymph (4). As all subjects had normal plasma triglyceride concentrations, VLDL will also have accounted for only a trace of apo B in plasma (2), removal of which, prior to immunoassay, would have incurred unavoidable losses of LDL. Our primary measure of HDL particle number was apo AI concentration. As apo AI is present in all HDLs and is unique to this lipoprotein class in fasted healthy humans, its concentration in plasma reflects HDL particle number (10, 40). As the number of apo AI molecules per particle varies, most containing three or four (41), and the relative proportions of different particles varies between subjects, the correlation between plasma apo AI concentration and HDL particle number in populations is nonlinear (42). However, this does not undermine our use of apo AI as a marker of the relative concentrations of HDL in plasma and lymph within subjects for calculating clearance rate, unless there is a preferential transfer of a specific HDL subclass across the endothelium. Although this possibility cannot be completely excluded, an absence of selective transport is supported by the fact that the apo AI/apo AII ratio in lymph was essentially identical to that in plasma (Table 2). Our earlier evidence that HDLs undergo remodeling in interstitial fluid (43) also does not affect the validity of our calculations. Unless significant remodeling occurs while the particles are in transit through intercellular pores, the total concentration of apo AI in lymph will reflect the rate at which HDL particles are entering interstitial fluid, whatever remodeling occurs after the event.

We used published data on the mean radii of LDL and HDL particles. Although both lipoprotein classes are discrete populations in healthy subjects, each is nevertheless also heterogeneous with respect to size owing to variations in core lipid content. The radii of 10.7 nm for LDL and 4.5 nm for HDL are the mean peak values recorded by NMR

in two population studies, one of 27,673 subjects (11) and another of 20,021 subjects (40). HDL size by NMR has been shown to agree with those by gradient gel electrophoresis (GGE) (10, 44) and compositional analysis (41). Published values for LDL radius by NMR have been identical to those by cryo-electron microscopy (45) and composition analysis (46), but to be smaller than that by GGE (10, 47). The reason for the larger value by GGE, which is not seen in the case of HDL, is not known, but may be owing to a charge effect. Furthermore, as Witte et al. (47) have pointed out, comparing average particle size by NMR with peak size by GGE is akin to comparing a mean and a mode.

It is pertinent to mention that the two-pore model of trans-endothelial transfer of proteins, although widely accepted, is a theoretical device that has not been visualized anatomically (23). The current view is that the dimensions of the small pores are determined by the spaces in the luminal glycocalyx (48–50), which lies in contact with plasma and overlies less selective channels through intercellular clefts (51, 52) and endothelial fenestrations (48). While the large pores have been suggested to be larger openings of intercellular clefts, transcellular channels formed by fusion of caveolae and small vesicles (53) are also contenders, with the advantage of providing the large pores with a fairly uniform diameter. Recent studies by Wagner et al. (54) using electron tomography showed that these structures are more common than once believed.

Our calculations assumed that the concentrations in lymph were those achieved when plasma-to-lymph transport has reached a steady-state. We endeavored to achieve steady state conditions by keeping the subjects supine for at least 8 h prior to the samples being taken. When Cooke et al. (55) measured lymph and plasma concentrations of albumin and apos in nine subjects over 4 days under conditions similar to those in the present study, lymph apo B concentration became constant shortly before midnight and remained so until 8:00 AM, when activity resumed. Furthermore, the rate at which lymph protein concentrations reach steady-state values following changes in microvascular fluid filtration should be inversely related to their volumes of distribution in the interstitial fluid. Because larger macromolecules have smaller volumes of distribution, they reach constant lymph concentrations more rapidly than smaller molecules (56).

It is reasonable to assume that our findings apply to all capillaries and venules with continuous endothelium. The specialized sinusoidal endothelia that are present in endocrine glands, liver, and spleen, for example, will be more permeable to lipoproteins. We did not measure transport across arterial endothelium, but a report (57) that the flux rates of labeled VLDL, LDL, and HDL into the aorta of rabbits were related inversely to their diameters suggests that ultrafiltration is the principal mechanism there also. If this is so, changes in endothelial permeability and lipoprotein particle size might affect the rate of development of atherosclerosis. According to the relation shown in Fig. 2, changes in LDL radius will have only a small effect on transport rate, but changes in HDL size, which commonly occur in response to disease, lifestyle change, drugs, and genetic factors, could have major effects. A decrease in the radius of an HDL particle from 4.5 to 4.0 nm, for example, would be expected to increase its transport rate by 38%, while an increase to 6.0 nm, a size seen in many subjects with familial cholesteryl ester transfer protein deficiency (58), would lower it by 12%. Such changes might have significant impacts on reverse cholesterol transport.

The authors thank the nursing staff of London Bridge Hospital for assistance with the lymph vessel cannulations.

REFERENCES

1. Chan, L. 1992. Apolipoprotein B, the major protein component of triglyceride-rich and low density lipoproteins. *J. Biol. Chem.* **267:** 25621–25624.
2. Contois, J. H., J. P. McConnell, A. A. Sethi, G. Csako, S. Devaraj, D. M. Hoefner, and G. R. Warnick. 2009. Apolipoprotein B and cardiovascular disease risk: Position statement from the AACC lipoproteins and vascular diseases division working group on best practices. *Clin. Chem.* **55:** 407–419.
3. Cheung, M. C., and J. J. Albers. 1984. Characterization of lipoprotein particles isolated by immunoaffinity chromatography: particles containing A-I and A-II and particles containing A-I but no A-II. *J. Biol. Chem.* **259:** 12201–12209.
4. Nanjee, M. N., C. J. Cooke, W. L. Olszewski, and N. E. Miller. 2000. Lipid and apolipoprotein concentrations in prenodal leg lymph of fasted humans. Associations with plasma concentrations in normal subjects, lipoprotein lipase deficiency, and LCAT deficiency. *J. Lipid Res.* **41:** 1317–1327.
5. Reichl, D., and J. J. Pflug. 1982. The concentration of apolipoprotein A-I in human peripheral lymph. *Biochim. Biophys. Acta.* **710:** 456–463.
6. Reichl, D., D. N. Rudra, and J. Pflug. 1989. The concentration of apolipoprotein A-II in human peripheral lymph. *Biochim. Biophys. Acta.* **1006:** 246–249.
7. Reichl, D., N. B. Myant, and J. J. Pflug. 1977. Concentration of lipoproteins containing apolipoprotein B in human peripheral lymph. *Biochim. Biophys. Acta.* **489:** 98–105.
8. Randolph, G. J., and N. E. Miller. 2014. Lymphatic transport of high-density lipoproteins and chylomicrons. *J. Clin. Invest.* **124:** 929–935.
9. Miller, N. E., C. C. Michel, M. N. Nanjee, W. L. Olszewski, I. P. Miller, M. Hazell, G. Olivecrona, P. Sutton, S. M. Humphreys, and K. N. Frayn. 2011. Secretion of adipokines by human adipose tissue in vivo: partitioning between capillary and lymphatic transport. *Am. J. Physiol. Endocrinol. Metab.* **301:** E659–E667.
10. Arsenault, B. J., I. Lemieux, J-P. Després, N-J. Wareham, E. S. G. Stroes, J. J. P. Kastelein, K-T. Khaw, and S. M. Boekholdt. 2010. Comparison between gradient gel electrophoresis and nuclear magnetic resonance spectroscopy in estimating coronary heart disease risk associated with LDL and HDL particle size. *Clin. Chem.* **56:** 789–798.
11. Mora, S., J. D. Otvos, N. Rifai, R. S. Rosenson, J. E. Buring, and P. M. Ridker. 2009. Lipoprotein particle profiles by nuclear magnetic resonance compared with standard lipids and apolipoproteins in predicting incident cardiovascular disease in women. *Circulation.* **119:** 931–939.
12. Martel, C., W. Li, B. Fulp, A. M. Platt, E. L. Gautier, M. Westerterp, R. Bittman, A. R. Tall, S. H. Chen, M. J. Thomas, et al. 2013. Lymphatic vasculature mediates macrophage reverse cholesterol transport in mice. *J. Clin. Invest.* **123:** 1571–1579.
13. Predescu, S. A., D. N. Predescu, and A. B. Malik. 2007. Molecular determinants of endothelial transcytosis and their role in endothelial permeability. *Am. J. Physiol. Lung Cell. Mol. Physiol.* **293:** L823–L842.
14. Grotte, G. 1956. Passage of dextran molecules across the blood-lymph barrier. *Acta Chir. Scand. Suppl.* **211:** 1–84.
15. Dehouck, B., L. Fenart, M-P. Dehouck, A. Pierce, G. Torpier, and R. Cecchelli. 1997. A new function for the LDL receptor: transcytosis across the blood-brain barrier. *J. Cell Biol.* **138:** 877–889.

16. Vlodavsky, I., P. E. Fielding, C. J. Fielding, and D. Gospodarowicz. 1978. Role of contact inhibition in regulation of receptor-mediated uptake of low density lipoprotein in cultured vascular endothelial cells. *Proc. Natl. Acad. Sci. USA.* **75:** 356–360.
17. Rosengren, B-I., O. Al Rayyes, and B. Rippe. 2002. Transendothelial transport of low-density lipoprotein and albumin across the rat peritoneum in vivo: effects of the transcytosis inhibitors NEM and filipin. *J. Vasc. Res.* **39:** 230–237.
18. Rutledge, J. C. 1992. Temperature and hydrostatic pressure-dependent pathways of low density lipoprotein transport across microvascular barrier. *Am. J. Physiol.* **262:** H234–H245.
19. Rutledge, J. C., F. E. Curry, P. Blanche, and R. M. Krauss. 1995. Solvent drag of LDL across mammalian endothelial barriers with increased permeability. *Am. J. Physiol.* **268:** H1982–H1991.
20. Cavelier, C., L. Rohrer, and A. von Eckardstein. 2006. ATP-binding cassette transporter A1 modulates apolipoprotein A-I transcytosis through aortic endothelial cells. *Circ. Res.* **99:** 1060–1066.
21. Cavelier, C., P. M. Ohnsorg, L. Rohrer, and A. von Eckardstein. 2012. The β-chain of cell surface F0F1 ATPase modulates apoA-I and HDL transcytosis through aortic endothelial cells. *Arterioscler. Thromb. Vasc. Biol.* **32:** 131–139.
22. Rohrer, L., P. M. Ohnsorg, M. Lehner, F. Landolt, F. Rinninger, and A. von Eckardstein. 2009. High-density lipoprotein transport through aortic endothelial cells involves scavenger receptor BI and ATP-binding cassette transporter. *Circ. Res.* **104:** 1142–1150.
23. Rippe, B., and B. Haraldsson. 1994. Transport of macromolecules across microvascular walls: two pore theory. *Physiol. Rev.* **74:** 163–219.
24. Taylor, A. E., and D. N. Granger. 1984. Exchange of macromolecules across the microcirculation. *In* Handbook of Physiology: Microcirculation. Vol. 4. I. E. Renkin and C. C. Michel, editors. American Physiological Society, Bethesda, MD. 467–520.
25. Nanjee, M. N., and N. E. Miller. 1996. Sequential microenzymatic assay of cholesterol, triglycerides and phospholipids in a single aliquot. *Clin. Chem.* **42:** 915–926.
26. Warren, H. B., P. Pantazis, and P. F. Davies. 1987. The third component of complement is transcribed and secreted by cultured endothelial cells. *Am. J. Pathol.* **129:** 9–13.
27. Rippe, B., and G. Stelin. 1989. Simulations of peritoneal solute transport during continuous ambulatory peritoneal dialysis (CAPD). Application of two pore formalism. *Kidney Int.* **35:** 1234–1244.
28. Anderson, J. L., and D. M. Malone. 1974. Mechanism of osmotic flow in porous membranes. *Biophys. J.* **14:** 957–982.
29. Levick, J. R., and C. C. Michel. 1978. The effects of position and skin temperature on the capillary pressures in the fingers and toes. *J. Physiol.* **274:** 97–109.
30. Mahy, I. R., J. R. Tooke, and A. C. Shore. 1995. Capillary pressure during and after incremental venous elevation in man. *J. Physiol.* **485:** 213–219.
31. Landis, E. M., and J. R. Pappenheimer. 1963. Exchange of substances through the capillary walls. *In* Handbook of Physiology: Circulation. Vol. 2. W. F. Hamilton, editor. American Physiological Society, Washington, DC. 961–1034.
32. Michel, C. C. Fluid movements through capillary walls. 1984. *In* Handbook of Physiology: Microcirculation. Vol. 4. I. E. Renkin and C. C. Michel, editors. American Physiological Society, Bethesda, MD. 375–409.
33. Curry, F. E. 1984. Mechanics and thermodynamics of transcapillary exchange. *In* Handbook of Physiology: Microcirculation. Vol. 4. I. E. Renkin and C. C. Michel, editors. American Physiological Society, Bethesda, MD. 309–374.
34. Michel, C. C., and M. E. Phillips. 1987. Steady state filtration at different capillary pressures in perfused frog mesenteric capillaries. *J. Physiol.* **388:** 421–435.
35. Renkin, E. M. 1964. Transport of large molecules across capillary walls. *Physiologist.* **60:** 13–28.
36. Breslow, J. L. 1985. Human apolipoprotein molecular biology and genetic variation. *Annu. Rev. Biochem.* **54:** 699–727.
37. Glass, C., R. C. Pittman, M. Civen, and D. Steinberg. 1985. Uptake of high-density lipoprotein-associated apolipoprotein A-I and cholesterol esters by 16 tissues of the rat in vivo and by adrenal cells and hepatocytes in vitro. *J. Biol. Chem.* **260:** 744–750.
38. Pittman, R. C., A. D. Attie, T. E. Carew, and D. Steinberg. 1979. Tissue sites of degradation of low density lipoprotein: Application of a method for determining the fate of plasma proteins. *Proc. Natl. Acad. Sci. USA.* **76:** 5345–5349.
39. Pittman, R. C., and D. Steinberg. 1984. Sites and mechanisms of uptake and degradation of high density and low density lipoproteins. *J. Lipid Res.* **25:** 1577–1585.
40. Parish, S., A. Offer, R. Clarke, J. C. Hopewell, M. R. Hill, J. D. Otvos, J. Armitage, and R. Collins; Heart Protection Study Collaborative Group. 2012. Lipids and lipoproteins and risk of different vascular events in the MRC/BHF Heart Protection Study. *Circulation.* **125:** 2469–2478.
41. Segrest, J. P., M. C. Cheung, and M. K. Jones. 2013. Volumetric determination of apolipoprotein stoichiometry of circulating HDL subspecies. *J. Lipid Res.* **54:** 2733–2744.
42. Mazer, N. A., F. Giulianini, N. P. Paynter, P. Jordan, and S. Mora. 2013. A comparison of the theoretical relationship between HDL size and the ratio of HDL cholesterol to apolipoprotein A-I with experimental results from the Women's Health Study. *Clin. Chem.* **59:** 949–958.
43. Miller, N. E., W. L. Olszewski, H. Hattori, I. P. Miller, T. Kujiraoka, T. Oka, T. Iwasaki, and M. N. Nanjee. 2013. Lipoprotein remodeling generates lipid-poor apolipoprotein A-I particles in human interstitial fluid. *Am. J. Physiol. Endocrinol. Metab.* **304:** E321–E328.
44. El Harchaoui, K., B. J. Arsenault, R. Franssen, J. P. Després, G. K. Hovingh, E. S. Stroes, and J. D. Otvos. 2009. High-density lipoprotein particle size and concentration and coronary risk. *Ann. Intern. Med.* **150:** 84–93.
45. Van Antwerpen, R., and J. C. Gilkey. 1994. Cryo-electron microscopy reveals human low density lipoprotein substructure. *J. Lipid Res.* **35:** 2223–2231.
46. Teerlink, T., P. G. Schaffer, S. J. L. Bakker, and R. J. Heine. 2004. Combined data from LDL composition and size measurement are compatible with a discoid particle shape. *J. Lipid Res.* **45:** 954–966.
47. Witte, D. R., M. R. Taskinen, H. Perttunen-Nio, A. van Tol, S. Livingstone, and H. M. Colhoun. 2004. Study of agreement between LDL size as measured by nuclear magnetic resonance and gradient gel electrophoresis. *J. Lipid Res.* **45:** 1069–1076.
48. Arkill, K. P., C. Knupp, C. C. Michel, C. R. Neal, K. Qvortrup, J. Rostgaard, and J. M. Squire. 2011. Similar endothelial glycocalyx structures in microvessels from a range of mammalian tissues: Evidence for a common filtering mechanism. *Biophys. J.* **101:** 1046–1056.
49. Michel, C. C., and F. E. Curry. 1999. Microvascular permeability. *Physiol. Rev.* **79:** 703–761.
50. Squire, J. M., M. Chew, G. Nneji, C. R. Neal, J. Barry, and C. C. Michel. 2001. Quasi-periodic substructure in the microvessel endothelial glycocalyx: a possible explanation for molecular filtering? *J. Struct. Biol.* **136:** 239–255.
51. Adamson, R. H., J. F. Lenz, X. Zhang, G. N. Adamson, S. Weinbaum, and F. E. Curry. 2004. Oncotic pressures opposing filtration across non-fenestrated rat microvessels. *J. Physiol.* **557:** 889–907.
52. Adamson, R. H., and C. C. Michel. 1993. Pathways through the intercellular clefts of frog mesenteric capillaries. *J. Physiol.* **466:** 303–327.
53. Simionescu, N., M. Simionescu, and G. E. Palade. 1975. Permeability of muscle capillaries to small hemepeptides. Evidence for the existence of patent transendothelial channels. *J. Cell Biol.* **64:** 586–607.
54. Wagner, R., S. Modla, F. Hossler, and K. Cymmek. 2012. Three-dimensional analysis and computer modelling of the capillary endothelial vesicular system with electron tomography. *Microcirculation.* **19:** 477–484.
55. Cooke, C. J., M. N. Nanjee, I. P. Stepanova, W. L. Olszewski, and N. E. Miller. 2004. Variations in lipid and apolipoprotein concentrations in human leg lymph: effects of posture and physical exercise. *Atherosclerosis.* **173:** 39–45.
56. Watson, P. D., and F. S. Grodins. 1978. An analysis of the effects of the interstitial matrix on plasma-lymph transport. *Microvasc. Res.* **16:** 19–41.
57. Stender, S., and D. B. Zilversmit. 1981. Transfer of plasma lipoprotein components and of plasma proteins into aortas of cholesterol-fed rabbits. Molecular size as a determinant of plasma lipoprotein influx. *Arteriosclerosis.* **1:** 38–49.
58. Arai, T., T. Tsukada, T. Murase, and K. Matsumoto. 2000. Particle size analysis of high density lipoproteins in patients with genetic cholesteryl ester transfer protein deficiency. *Clin. Chim. Acta.* **301:** 103–117.